University of California

NSG-91-60

52p

UNPUBLISHED PRELIMINARY DATA

N64-16760

CODE-1

CR-53114

OTS PRICE

XEROX $ 5.60 ph.

MICROFILM $ 1.76 mf.

UNIVERSITY OF CALIFORNIA U.,
SANTA BARBARA

# Reflectivity of Solids in the Vacuum Ultraviolet

A Thesis submitted in partial satisfaction
of the requirements for the degree of

MASTER OF ARTS

in

PHYSICS

by

John Osantowski (M.A. Thesis)

May, 1963 52 p

(NASA Grant NsG-91-60)
(NASA CR-53114
OTS: $5.60 ph, $1.76 mf

The thesis of John F. Osantowski is approved:

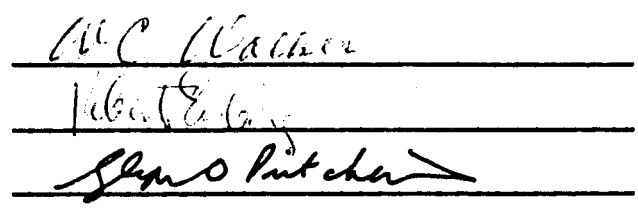

Committee

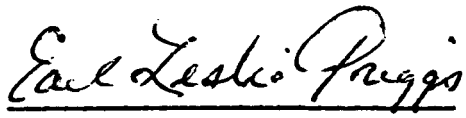

Dean, Graduate Division

## Abstract

REFLECTIVITY OF SOLIDS IN THE VACUUM ULTRAVIOLET

16760 John F. Osantowski A

Peaks observed in the reflection spectrum of several solids beyond the fundamental absorption edge have been attributed to direct interband transitions at symmetry points in the Brillouin zone. In this work a special vacuum reflectometer was constructed and the reflectivity of cubic single crystal zinc sulphide was measured between 4 and 30 electron volts. Prominent reflectivity peaks were observed at 5.9, 7.2, 9.8, and 13.8 electron volts. The first three peaks were tentatively attributed to the $\Lambda_3 \rightarrow \Lambda_1$, $\Sigma_4 \rightarrow \Sigma_1$, and $L_3 \rightarrow L_3'$ transitions respectively. This assignment was made by comparing the reflectivity of zinc sulphide with similar data and electron energy band calculations for germanium. The peak at 13.8 electron volts was attributed to a transition from the d-band, and this excitation energy was found to compare favorably with that obtained for zinc selenide.

AUTHOR

TABLE OF CONTENTS

# CHAPTER I

## Introduction

Improved techniques for the calculation of electron energy bands in solids have been applied recently by several investigators[1] to various classes of solids such as the group IV elements Ge and Si, the III - V compounds InSb and GaP, and the II - VI compounds ZnS and CdS. These advances have prompted extensive experimental activity directed toward verifying the theoretical results. Studies of the optical properties of solids in the spectral region corresponding to direct electronic transitions between the energy bands afford an excellent means of verifying certain aspects of the theory. Such studies, however, have until recently been limited to the spectral region in the vicinity of the lowest lying interband transition which normally occurs in the infrared or visible region of the spectrum. In order to provide a more detailed verification of band calculations it is important to extend these measurements to considerably higher energy. In the present experiment, optical studies of ZnS single crystals were carried out in the energy range encompassing several prominent interband transitions.

The group IV elements crystallize into the diamond

structure, and the III - V compounds crystallize into the zinc blend form. Group II - VI solids exhibit two forms, zinc blend and hexagonal. No extensive band structure calculations have been performed for the II - VI compounds in the zinc blend form; however, Herman and Skillman[1] have carried out preliminary calculations for hexagonal zinc sulphide. Since all three groups have the face centered cubic space lattice in common, however, the band structure for all solids with the diamond or zinc blend structure should be closely related.

Investigations of the optical properties of these solids for the specific purpose of verifying the results of band calculations and for observing intercompound similarity in band structure have been carried out with success by several investigators for the group IV and III - V compounds.

Similar studies of the zinc blend, II - VI, materials have been made, and the results have been interpreted by assuming a band structure similar to the group IV and III - V solids.

Jahoda[2] has measured the reflectivity of barium oxide single crystals in the region of the fundamental absorption edge. From these measurements he was able to calculate values for the absorption coefficient. Reflectivity measurements, however, pose certain difficulties.

They are in general quite sensitive to the surface condition of the sample. Chemical action, adsorption of impurities, or mechanical defects may alter the reflectivity significantly. For this reason, freshly cleaved or polished and etched samples are preferred. Jahoda, using samples cleaved in vacuum, obtained values for the absorption coefficient in good agreement with transmission measurements. It was also observed that the structure of the curve for the absorption coefficient is directly correlated to the structure of the curve for the reflectivity. Therefore, the position of absorption bands may be determined directly from the reflectivity measurement. It was also concluded that the interpretation of reflectivity measurements is a valid method for determining the optical properties.

The measurement of the reflectivity for the group IV and III - V solids, InSb, InAs, GaAs, GaP, Ge, Si, and C beyond the fundamental edge yields a number of prominent reflectivity peaks. These peaks have been assigned by Ehrenreich, Philipp and Phillips[3,4] to direct interband transitions at symmetry points in the Brillouin zone. The energies at which these peaks were observed compare very favorably with the results of band calculations. The reflectivity of the II - VI solids is, as expected,

quite similar to that for the group IV and III - V materials. Using this similarity Cardona[5] has identified several of the reflectivity peaks for ZnSe, ZnTe, CdTe, HgTe and HgSe in the region below 5 electron volts.

The prototype II - VI solid, ZnS, has a fundamental absorption edge at approximately 3.7 electron volts, and no additional structure is observed below the edge. It was decided, therefore, to measure the reflectivity of this material in the energy range of 4 to 30 electron volts. This important solid has been omitted from previous work because the spectral region involved occurs in the vacuum ultraviolet where special experimental methods must be employed. In the present experiment, the reflectivity was measured over a broad spectral region with apparatus designed and assembled for operation throughout the vacuum ultraviolet region.

## CHAPTER II

## Experimental Apparatus and Procedure

The experimental equipment consisted of an ultraviolet light source, a vacuum monochromator, and a reflectometer. Radiation generated in the source was passed through a slit system onto the diffraction grating of the monochromator and the dispersed beam was focussed on an exit slit. By rotating the grating about a vertical axis, the spectrum was swept past the slit. Thus, a nearly monochromatic beam passed into the reflectometer and onto the sample. The light reflected from the sample was collected by a light pipe and transmitted to a photomultiplier. The output of the photomultiplier was monitored by a micromicroammeter which in turn drove a chart recorder. A recorded trace of the reflected and incident radiation could thus be obtained. The reflectivity of the sample was calculated by comparing the peak heights of the two traces. In the following sections the apparatus and experimental procedure are described in detail.

The ultraviolet light source used was similar to that developed by Walker[6] et al. and is illustrated in figure 1. It consists of a ceramic discharge tube with a 3 mm x 4 cm capillary. Gas at reduced pressures was passed into the tube through a water-cooled, vacuum-sealed cap. The

discharge tube was connected to a differential pumping chamber which was evacuated by a 140 liter per minute mechanical pump. The differential pumping chamber and light source were isolated from the remaining parts of the system by a 2" diameter vacuum gate valve located in the entrance slit arm of the monochromator. A vacuum thermocouple gauge located in the differential pumping chamber was used to monitor the gas pressure in the light source.

A direct current glow discharge in hydrogen gave rise to two distinct spectral regions. They consisted of a many-lined atomic and molecular spectrum extending from 7 to 14 electron volts, 1700 to 900 Å, and a molecular continuum extending from 4 to 7 electron volts, 3200 to 1700 Å. During the measurements, the discharge was allowed to operate for approximately 30 minutes after firing to insure that any change in light intensity due to removal of impurities was minimized. The reproducibility of the spectrum was estimated to be ± 5% over periods of several hours. Typical operating conditions for this source are given in table I. A high voltage, low pressure pulsed discharge in argon was used for the spectral region of 12 to 30 electron volts, corresponding to the wave length region between 1000 and 400 angstroms. The discharge was maintained by alternately discharging two 0.1 mfd capacitors

through the gas with a rotary spark gap. The capacitors were charged to between 5 and 10 kilovolts with a high voltage d.c. power supply. A discharge repetition rate of 60 per second and a pulse duration of approximately 100 microseconds were typical of this mode of operation. This source yields primarily strong emission lines of multi-ionized atoms. The wave lengths of the lines used were obtained by comparison with tabulated spectrum tables[7] and they are listed in table II. Impurity lines generated in this source have a tendency to decrease in intensity as the source is operated; however, the primary lines were observed to remain constant to about ± 5%. Typical operating conditions of this source are listed in table I.

The vacuum monochromator used was a 0.5 meter Seya-Namioka mounting constructed by the Jarrell Ash Company. A Bausch and Lomb grating ruled at 1200 lines per mm over an area 50 x 30 mm was installed in the monochromator. The grating was blazed at 1500 Å and overcoated with magnesium fluoride to increase the efficiency in the ultraviolet. For most of the measurements an exit slit width of 100 microns giving a band pass of about 2Å was used.

The monochromator was evacuated by a 3" oil diffusion pump backed by a 140 liter per minute mechanical pump. An ultimate pressure of $10^{-6}$ torr was obtained when liquid

nitrogen vapor traps were used.

Wave length scanning was obtained by rotating the grating with a twelve speed electric drive which provided various scanning rates from 5 to 2500 Å per minute. A wavelength indicating counter which reads directly in angstrom units was attached to the drive mechanism. Data were normally taken at scanning rates of 25 and 50 Å per minute.

The special vacuum reflectometer constructed for this experiment is shown in figures 2 and 3. It consisted of a 6" diameter seamless stainless steel vacuum chamber which was attached to the exit slit of the monochromator through a 2" high vacuum gate valve. Reduced pressure was maintained in the chamber by a 2" oil diffusion pump backed by a 140 liter per minute mechanical pump. Ultimate pressures attainable with liquid nitrogen cold traps varied from $10^{-6}$ to $5 \times 10^{-7}$ torr. The primary components of the reflectometer were a double cold trap, a sample holder, a light pipe,[8] and a photomultiplier assembly.

The double cold trap, as indicated in figure 2, was completely removable from the main chamber for cleaning and alignment purposes. The outer trap was constructed so that it extended into the main chamber. For actual low temperature measurements, an aluminum shield, shown by the dashed line in figure 2, which surrounded the sample

holder was attached to the outer trap. In this manner the area surrounding the sample was trapped while the sample remained at room temperature. The inner trap was not filled until the outer trap had cooled for a sufficient length of time. The bottom of the inner trap was constructed of copper for maximum thermal conductivity. Tests made with a thermocouple attached to the bottom of the aluminum shield showed that it reached a temperature of 90 degrees K within approximately 60 minutes after the trap was filled with liquid nitrogen. Although no temperature measurements were taken at the sample holder, it assuredly reached a temperature below 90 degrees K.

A copper sample holder was constructed with two identical faces. Each face had been accurately milled to hold the sample at 20 degrees from normal incidence and a hole the size of the radiation beam was located in the center of each face. The sample was held to one face with a bronze clamp which also served to mask all but that portion of the sample exposed to the direct beam. This precaution insured that no scattered light was reflected by the sample into the light pipe. The sample was inserted or removed from the beam by rotating the inner cold trap through 90 degrees. All parts of the sample holder were chemically darkened to decrease spurious reflections. Tests to observe light scattered from either face were made by rotating the

light pipe to the forward position. The scattered light intensity was found to be negligible. The beam was also measured as it passed through each face of the holder and no significant difference was observed. It was, therefore, assumed that the sample holder did not interfere with the reflection measurements in any way.

A light pipe was constructed of 10 mm pyrex glass rod bent into a hook shape and sealed to the reflectometer with O-rings as shown in figures 2 and 3. Each face of the light pipe was polished to optical quality to give maximum light transmission. When rotated as shown in figure 2, the face of the light pipe intercepted the incident or the reflected beams. In order to detect the ultraviolet radiation, a fluorescent coating of sodium salicylate was placed on the face of the light pipe. The fluorescent efficiency of this material has been measured by several investigators[8, 9] and found to be constant over a wide spectral region. The center of its fluorescent band occurs at 4300 Å and is therefore easily transmitted by the light pipe. The opposite end of the light pipe was sealed into a light tight photomultiplier housing which held it approximately 1/32" from the face of the photomultiplier.

An EMI 6256B photomultiplier which has a maximum sensitivity near 4300 Å was used. A divider voltage for the

tube was supplied by a Victoreen model 1HVN variable d.c. power supply which was normally operated at 1000 volts giving about 70 volts per stage on the photomultiplier. Dark currents observed with this voltage were less than $10^{-10}$ amperes and were negligible compared to the photo current generated by the light signal. The photocurrent was measured with a Keithley model 410 micro-microammeter which in turn drove a 10 millivolt Leeds and Northrup model S chart recorder whose gain was adjusted for minimum noise and maximum response to the micro-microammeter.

Optical alignment of the reflectometer was obtained by replacing the light source with an incandescent lamp and using the central image of the monochrometer. The sample holder was first adjusted until the light beam passed freely through each face. A sample was then positioned in the holder and the horizontal position of the light pipe was varied until the beam was intercepted at the same region of the coated face in either position. The entire system was then sealed and evacuated as soon as possible after the sample was installed. When taking the measurements both the incident and reflected beam were positioned on the light pipe by setting the monochromator on a prominent line in the spectrum and rotating the light pipe for maximum signal. The position for maximum signal was always found to be sharp, which indicated that the light

beam was not scattered by the sample holder and was specularly reflected by the sample. Since the optical path in either position was identical, the measurements yielded absolute values for the reflectivity.

## CHAPTER III

## Theoretical Considerations

The classical description of the interaction of electromagnetic radiation with solids is given by the solution of Maxwell's equations. A detailed discussion of this problem is presented in most standard references on the optical properties of solids,[10,11] and the following discussion is a summary of the results.

The plane wave solution of the wave equation for a material with a finite conductivity is characterized by a complex dielectric constant

$$\varepsilon(\omega) = \varepsilon_1(\omega) + i\,\varepsilon_2(\omega) \qquad (1.)$$

The real and imaginary parts of $\varepsilon(\omega)$ are related to the index of refraction $n$ and the extinction coefficient $k$ by:

$$\varepsilon_1(\omega) = n^2 - k^2 \qquad (2a.)$$

$$\varepsilon_2(\omega) = 2nk \qquad (2b.)$$

The extinction coefficient is a measure of the attenuation of the wave as it penetrates the solid and is related to the absorption coefficient $\alpha$ by

$$\alpha = \frac{2\omega k}{c} \qquad (3.)$$

where $\omega$ is the frequency of the wave and $c$ is the speed of light. The imaginary part of $\varepsilon(\omega)$ is related to absorption processes in the solid, and an expression for $\varepsilon_2(\omega)$ in

terms of $\alpha$ can be obtained from equations (2b) and (3):

$$\varepsilon_2(\omega) = \frac{nc}{\omega}\alpha \qquad (4.)$$

The complex amplitude of reflection and the reflectivity are given by equations (5) and (6) respectively.

$$r = \frac{n - ik - 1}{n - ik + 1} \qquad (5.)$$

$$R = |r|^2 = \frac{(n-1)^2 + k^2}{(n+1)^2 + k^2} \qquad (6.)$$

It is customary to write the complex amplitude in the form:

$$r = \rho e^{iQ}$$

where

$$\rho^2 = R \qquad (7.)$$

and $Q$ is the phase. Taking the logarithm of (7), the following complex function is formed:

$$\ln r = \ln \rho - iQ \qquad (8.)$$

The phase angle can be found as a function of frequency by applying the Kramers-Kronig dispersion relation to (8). This yields the expression:

$$Q(\omega) = \frac{1}{2\pi}\int_0^\infty \ln\left(\frac{\omega' - \omega}{\omega' + \omega}\right)\frac{d}{d\omega'}\ln R(\omega')\, d\omega' \qquad (9.)$$

which requires a knowledge of the reflectivity over an extended frequency range. It is therefore necessary to employ an extrapolation method to determine the reflectivity for zero and infinite frequencies. The integration of

equation (9) can be done by graphical or numerical methods. By equating the real and imaginary parts of (5) and (7), the following expressions for $n$ and $k$ in terms of $\rho$ and $\theta$ are obtained:

$$n = \frac{1-\rho^2}{1+\rho^2-2\rho\cos\theta} \qquad (10a.)$$

$$k = \frac{2\rho\sin\theta}{1+\rho^2-2\rho\cos\theta} \qquad (10b.)$$

This analysis provides one method for determining $\varepsilon_1(\omega)$ and $\varepsilon_2(\omega)$ from a measurement of the reflectivity over an extended frequency range. It is an especially useful method for determining the absorption properties of a solid in a region where direct absorption measurements become impractical.

An expression, based on the one electron Bloch model, for the absorption coefficient $\alpha$ or $\varepsilon_2(\omega)$, the imaginary part of the dielectric constant, in the interband transition region can be obtained by generalizing the argument given by Smith.[12] Let the states in the valence band and conduction band be specified by the Bloch functions

$$\psi_v(\vec{k},\vec{r}) = V^{-1/2} u_v(\vec{k},\vec{r})\, e^{i\vec{k}\cdot\vec{r}}$$

$$\psi_c(\vec{k}',\vec{r}) = V^{-1/2} u_c(\vec{k}',\vec{r})\, e^{i\vec{k}'\cdot\vec{r}}$$

where $\vec{k}$ is the wave vector for a particular electronic state in the band, and $V$ is the volume of the crystal. The functions $u(\vec{k},\vec{r})$ have the periodicity of the direct lattice. The incoming monochromatic wave is specified by a vector potential

$$\vec{A} = \hat{a}_0 A_0 e^{i(\vec{K}\cdot\vec{r} - \omega t)} \qquad (12.)$$

and is treated as a periodic perturbation on the Bloch states. The perturbation operator is given by

$$H = \frac{iek}{m} A_0 e^{i\vec{K}\cdot\vec{r}} \hat{a}_0 \cdot \nabla \qquad (13.)$$

where $e$ is the electronic charge and $m$ the free electron mass. The matrix elements for the interaction operator are

$$H_{cv} = \langle c | H | v \rangle \qquad (14.)$$

and the interband momentum matrix elements are

$$\vec{p}_{cv} = -ik \langle c | \nabla | v \rangle \qquad (15.)$$

Matrix elements for $H$ may be expressed in terms of the interband momentum matrix elements:

$$H_{cv} = -\frac{eA_0}{m} \hat{a}_0 \cdot \vec{p}_{cv} \qquad (16.)$$

These matrix elements are found to be zero unless the condition

$$\vec{k}' - \vec{k} = 0 \qquad (17.)$$

is satisfied. Therefore, if a transition from the valence to the conduction band occurs, the wave vector in the initial and final states must be the same. Such transitions are called vertical or direct interband transitions. The transition rate for transitions between the valence and conduction bands is:

$$\gamma_{cv} = \frac{2\pi}{\hbar} |H_{cv}|^2 \delta(E_c - E_v + \hbar\omega) \qquad (18.)$$

where

$$|H_{cv}|^2 = \frac{e^2 A_0^2}{m^2} |\hat{q}_0 \cdot \vec{p}_{cv}|^2 \qquad (19.)$$

and

$$\delta(E_c - E_v + \hbar\omega) = 0 \quad \text{if } E_c \neq E_v + \hbar\omega$$
$$= 1 \quad \text{if } E_c = E_v + \hbar\omega \qquad (20.)$$

$E_v$ and $E_c$ are the energies of the states in the valence and conduction bands respectively, and $\hbar\omega$ is the energy of the absorbed photon. The probability for

absorption of a photon per unit time per unit volume is found by summing $r_{cv}$ over all allowed states and is given by:

$$P_{cv}(\hbar\omega) = \frac{V}{4\pi^3}\int_{\vec{k}'=\vec{k}} r_{cv}\, d\vec{k} \qquad (21.)$$

This volume integral in $\vec{k}$ space may be written in terms of the surface integral

$$P_{cv}(\hbar\omega) = \frac{V}{4\pi^3}\int_S r_{cv}\frac{dS\, d(E_c - E_v)}{|\nabla_k(E_c - E_v)|} \qquad (22.)$$

where the integration is taken over the surface in space identified by:

$$E_c - E_v = \text{constant} \qquad (23.)$$

Inserting (18) and (19) into (22) $P_{cv}(\hbar\omega)$ becomes:

$$P_{cv}(\hbar\omega) = \frac{V}{4\pi^3}\frac{2\pi}{\hbar}\frac{e^2A_0^2}{m^2}\int |\hat{q}_0\cdot\vec{p}_{cv}|^2\,\delta(E_c - E_v - \hbar\omega)\frac{dS\, d(E_c - E_v)}{|\nabla_k(E_c - E_v)|} \qquad (24.)$$

The surface integral:

$$\frac{V}{4\pi^3}\int_S \frac{dS}{|\nabla_k(E_c - E_v)|} \qquad (25.)$$

is an expression for the number of states per unit volume separated by an energy difference $E_c - E_v$ . This is referred to as the joint density of states and is denoted by $\rho(\Delta E_{cv})$ . Therefore,

$$P_{cv}(\hbar\omega) = \frac{2\pi}{\hbar}\frac{e^2 A_0^2}{m^2}\int |\vec{a}_0 \cdot \vec{P}_{cv}|^2 \delta(E_c - E_v + \hbar\omega)\rho(\Delta E_{cv})\,d(E_c - E_v) \tag{26.}$$

Integrating (26) yields

$$P_{cv}(\hbar\omega) = \frac{2\pi}{\hbar}\frac{e^2 A_0^2}{m^2}|\vec{a}_0 \cdot \vec{P}_{cv}|^2 \rho(\hbar\omega) \tag{27.}$$

as the final expression for the absorption of a photon with energy $\hbar\omega$ per unit volume per unit time. The absorption coefficient is given in terms of $P_{cv}(\hbar\omega)$ by:

$$\alpha = \frac{P_{cv}(\hbar\omega)}{F} \tag{28.}$$

where $F$ is the photon flux in the material. This flux is given by:

$$F = \frac{c n \varepsilon_0 \omega}{2\hbar} A_0^2 \tag{29.}$$

Combining (27), (28) and (29), the absorption coefficient

for valence to conduction band transitions is:

$$\alpha = \frac{4\pi e^2}{m^2 c n \varepsilon_0 \omega} \left| \hat{a}_0 \cdot \vec{p}_{cv} \right|^2 \rho(\hbar\omega) \qquad (30.)$$

An oscillator strength for the transition may be defined as:

$$f_{cv} = \frac{2 \left| \hat{a}_0 \cdot \vec{p}_{cv} \right|^2}{m \hbar \omega} \qquad (31.)$$

and in terms of $f_{cv}$ equation (30) becomes

$$\alpha = \frac{2\pi e^2 \hbar}{m \varepsilon_0 c n} f_{cv} \rho(\hbar\omega) \qquad (32.)$$

An expression for $\varepsilon_2(\omega)$ can be found from equation (4).

$$\varepsilon_2(\omega) = \frac{2\pi e^2 \hbar}{m \varepsilon_0 \omega} f_{cv} \rho(\hbar\omega) \qquad (33.)$$

Band calculations for Ge performed by Brust, Phillips and Bassani[13] have shown that the interband momentum matrix elements are approximately $\vec{k}$ independent. Therefore, the structure in $\varepsilon_2(\omega)$ is primarily due to the joint density of states. As can be seen from equation (25), the joint density of states has

singularities when the condition

$$\nabla_k (E_c - E_v) = 0 \qquad (34.)$$

is satisfied. This can occur in two ways, either

$$\nabla_k E_c = \nabla_k E_v \qquad (35a.)$$

or

$$\nabla_k E_c = \nabla_k E_v = 0 \qquad (35b.)$$

These singularities manifest themselves as maxima $M_3$, minima $M_0$ or saddle points, $M_1$ or $M_2$, in $\rho(\Delta E_{cv})$. Structure in the experimentally determined values of $R(\omega)$ or $\varepsilon_2(\omega)$ may be correlated with these singularities to give information on the location of the various energy gaps observed.

## CHAPTER IV

## Experimental Results and Interpretation

The reflectivity measured for two samples of single crystal zinc sulphide is shown in figures 4 and 5. The single crystal samples were obtained by cleaving a large single crystal which was purchased from the Eagle-Picher Company of Cleveland. Only those cleavages which were smooth over an area approximately the size of the beam were used for measurement. The crystal designated in figure 4 as sample I was mounted in the reflectometer and kept under vacuum during the entire measurement process. Sample II was allowed to remain in air for about thirty days before measurement. Decreased reflectivity for sample II was attributed to the absorption of impurities on its surface. It is significant that the structure of the reflection spectrum, however, is identical for each sample. The curves in figures 4 and 5 represent the average of several sets of data taken over points with a spacing of approximately 0.20 electron volts and the reflectivities shown are estimated to be accurage to $\pm$ 2%. In the region from 20 to 29 electron volts the reflectivity was found to be low and relatively constant. Data were plotted only at a few selected wave lengths to obtain the general trend of the curve. Prominent peaks observed in the reflection spectrum are summarized in table III. Peak $E_1$ showed evidence of a

shoulder at 5.6 ev which was, however, within the scattering of the data in this region and was therefore omitted from the smoothed curve. The reflection spectrum of ZnS is very similar to that obtained by Ehrenreich and Phillipp[4] for germanium which is shown in figure 6. It is also similar to that of other group IV and group III-V solids.

The peaks $E_1$, $E_2$, and $E_3$ were tentatively identified by comparison with the band structure calculations of Brust, Phillips and Bassani[14] for germanium. These authors obtained the electronic energy bands of germanium along the (100), (111), and (110) directions in the Brillouin zone. A reproduction of their results is shown in figure 7 in which transitions are indicated at points satisfying conditions (35a) and (35b). A summary of the interband transitions identified by Brust, Phillips and Bassani is given in table IV. The peaks in the room temperature reflectivity for germanium, shown in figure 5, were labeled, using this table. Fine structure, of course, is not resolved in this curve. By comparing the present results on zinc sulphide with those for germanium, $E_1$ can be assigned to a $\Lambda_3 \rightarrow \Lambda_1$, $E_2$ to a $\Sigma_4 \rightarrow \Sigma_1$, and $E_3$ to a $L_3 \rightarrow L_3'$ transition. At present, this identification is tentative. A more positive determination can only be made after low temperature measurements and refined band structure calculations are available.

Reflectivity peaks observed for the III-V solids GaP, GaAs, InAs, and InSb for energies greater than 10 ev have been attributed by Ehrenreich and Philipp[15] to direct transitions from the d-band to the bottom of the conduction band. The d-band occurs several electron volts below the valence band and is assumed to be due to the d-shell electrons of the group II or III element of the solid. Reflectivity data for silicon, which lacks d-shell electrons, exhibits no structure beyond 10 ev. Figure 8, taken from reference 4, is a plot of the d-band excitation energy in the solids GaAs, GaP, and ZnSe versus the corresponding atomic transition $3d^{10} \rightarrow 3d^{9}4p$ for the completely ionized atom. Since the curve is linear, it can be assumed that the same transition is responsible in each case. The peak $E_4$ obtained in the present study for zinc sulphide has been included in figure 8. As this peak falls exactly on the straight line, it was attributed to a d-band transition. The weak dependence of the d-band to conduction band energy gap in zinc compounds is shown by the agreement of the present value of 13.8 ev for ZnS with that of 14 ev for ZnSe.

## CONCLUSION

The reflection spectrum of cubic single crystal zinc sulphide was measured in the energy region between 3 and 30 electron volts. Four prominent reflectivity peaks were observed and identified as direct interband transitions. The peaks, $E_1$, $E_2$ and $E_3$, were associated with valence to conduction band transitions at critical points in the Brillouin zone. This assignment was made by comparing the reflectivity of zinc sulphide with similar data and electron energy band calculations for germanium. The identification of these peaks in zinc sulphide, however, must remain tentative until the reflectivity is measured at liquid nitrogen and possibly liquid helium temperatures. Additional structure observed in this temperature region should make the assignment of the transitions by this comparison method more definite. Unambiguous identification of these peaks in zinc sulphide and in other II-VI solids can be made only with the aid of extensive band calculations for these materials.

The remaining reflectivity peak, $E_4$, observed in zinc sulphide was attributed to a d-band transition. Peaks in the II-VI solids, ZnTe and ZnSe, at approximately the same energy, and the linear relationship between the d-band excitation energy in the solid and the energy of the corresponding atomic transitions for these and several III-V

solids, firmly substantiate this identification. Additional structure in the d-band due to transitions terminating at different conduction band levels should be expected. An investigation of the d-band at both room and low temperatures with a high resolution instrument is presently planned.

Although the present data are suitable for Kramers-Kronig analysis, such an analysis has not yet been carried out. The importance of this analysis is greatly increased if applied to measurements made at low temperatures. Reflection measurements at 80 degrees K are currently being attempted for several solids, ZnS, ZnSe, CdS and diamond. However, with the present reflectometer, the rate of adsorption of impurities on the surface of the sample at liquid nitrogen temperature is prohibitive. The reflectivity is found to decrease by a factor of 80% in approximately ten minutes after the sample is first cooled. Oil vapor from the vacuum pumps is thought to be the primary impurity present. A new reflectometer with more effective liquid nitrogen traps and utilizing an ion vacuum pump is now under consideration.

# APPENDIX I

## Tables and Figures

Table I

| Source | Pressure in Light Source | Pressure in Monochromator | Pressure in Reflectometer | Operating Voltage |
|---|---|---|---|---|
| Hydrogen | 1 torr | $4\text{-}5 \times 10^{-4}$ torr | $5 \times 10^{-5}$ torr | 1000 V |
| Argon | $5 \times 10^{-2}$ | $2\text{-} \times 10^{-4}$ | $10^{-5}$ | 6000 V |

TYPICAL OPERATING CONDITIONS OF THE ULTRAVIOLET LIGHT SOURCES

Table II

Argon Spectrum Wavelength Identification

| Nominal λ(Å) | Tabulated spectral lines (Å) | |
|---|---|---|
| 446.8 | 446.0 AV | |
| | 447.0 AV | |
| | 447.5 AV | |
| 457.9 | 457.0 AVI | |
| | 457.5 AVI | |
| | 459.3 AVI | |
| 462.3 | 461.2 AV | 462.0 OVI |
| | 463.9 AV | 462.2 OVI |
| | 462.4 AV | |
| 468.2 | 466.5 AIII | 469.0 OIII |
| | 467.4 AIII | 469.8 OIII |
| | **468.5 AIII** | |
| 473.2 | 470.0 AIII | 475.7 AVII |
| | 473.0 AIII | |
| | 473.9 AIII | |
| 478.4 | 476.4 AIII | 479.4 AVII |
| | | 479.5 AVII |
| 483.5 | 481.9 AIII | 484.1 AIII |
| | 482.6 AIII | 485.2 AIII |
| 488.8 | 487.0 AIII | 488.8 AII |
| | 488.0 AIII | 491.1 AIII |
| | 488.5 AIII | |
| 492.2 | 492.2 AIII | |
| 500.4 | 499.9 AII | |
| | 500.8 AII | |
| 503.5 | 502.0 AII | 504.8 AII |
| | 502.2 AII | 505.0 AII |
| | 503.6 AII | |

Table II (continued)

| Nominal λ(Å) | Tabulated spectral lines (Å) | | |
|---|---|---|---|
| 508.0 | 508.4 AIII | 507.4 OIII | |
| | 508.6 AIII | 507.7 OIII | |
| | | 508.0 OIII | |
| 516.3 | 515.5 OII | | |
| | 515.6 OII | | |
| | 517.9 OII | | |
| 519.6 | 518.9 AII | 522.1 AV | 518.2 OII |
| | 519.3 AII | | |
| 525.0 | 522.8 AII | 525.8 OIII | |
| | 524.7 AII | | |
| | 526.5 AII | | |
| 530.7 | 529.9 AIII | 530.5 AII | 529.9 NII |
| | 532.4 AIII | | |
| 534.7 | 536.8 AIII | 533.5 NII | |
| | 535.6 AIII | 533.6 NII | |
| | 537.1 AII | 533.6 NII | |
| | | 533.7 NII | |
| | | 533.8 NII | |
| 538.7 | 538.8 AIII | 537.8 OII | |
| | 537.5 AIII | 538.3 OII | |
| | | 538.3 OII | |
| | | 539.1 OII | |
| | | 539.5 OII | |
| | | 539.9 OII | |
| 543.3 | 542.9 AII | | |
| | 543.2 AII | | |
| | 543.7 AII | | |
| 547.2 | 544.7 AVI | 546.2 AII | |
| | | 547.2 AII | |
| | | 547.5 AII | |
| 550.2 | 551.4 AVI | 548.8 AII | |
| | | 550.5 AII | |

Table II (continued)

| Nominal λ(Å) | Tabulated spectral lines (Å) | | |
|---|---|---|---|
| 555.7 | 553.5 AIII<br>556.9 AIII | 555.6 AVI<br>556.8 AII | |
| 559 | 560.2 AII<br>558.3 AIII | 558.5 AV | |
| 567 | | | |
| 573.9 | 576.7 AII<br>572.0 AII<br>573.4 AII | 573.5 AIII | |
| 578.4 | 578.1 AII<br>578.6 AII | 578.4 AIII | |
| 582.7 | 583.4 AII<br>580.3 AII | 580.4 OII<br>581.0 OII | 585.6 AVII |
| 593 | | | |
| 599.3 | 597.8 OIII<br>599.6 OIII | 600.6 OII | |
| 602.9 | 602.9 AII | | |
| 606.3 | 604.2 AIII<br>608.4 OIV | | |
| 610.8 | 612.6 AII<br>609.8 OIV | 610.0 OIII<br>610.8 OIII | |
| 616.7 | 616.3 OII<br>616.4 OII | 616.9 OIV<br>617.0 OIV | |
| 624.8 | 623.8 AIII | 624.6 OIV<br>625.1 OIV<br>625.8 OIV | |
| 636.3 | 637.3 AIII<br>635.2 NII | | |
| 643.9 | 641.8 AIII<br>643.3 AIII | 644.6 NII<br>645.2 NII<br>644.8 NII | |

Table III

| Peak | | |
|---|---|---|
| $E_1$ | 5.9 e.v. | 2530 Å |
| $E_2$ | 7.2 | 1720 |
| $E_3$ | 9.8 | 1265 |
| $E_4$ | 13.8 | 900 |

PROMINENT PEAKS

in the

REFLECTION SPECTRUM OF ZnS

Table II (continued)

| Nominal λ(Å) | Tabulated spectral lines (Å) | | |
|---|---|---|---|
| 653 | | | |
| 665.3 | 664.6 AII<br>666.0 AII | | |
| 671.9 | 670.9 AII<br>671.9 AII | 671.4 NII<br>671.8 NII<br>671.0 NII<br>671.6 NII<br>672.0 NII | 672.9 OII<br>673.8 OII |
| 683.3 | 683.3 AIV | | |
| 685.7 | 685.0 NII<br>685.5 NII | 685.8 NII<br>686.3 NII | |
| 689.2 | 688.4 AIV<br>689.0 | 690.2 AIII | |
| 695.5 | 695.5 AIII | | |
| 699.9 | 700.3 AIV<br>699.4 AIV | | |
| 703.0 | 702.3 OIII<br>702.8 OIII | 702.9 OIII<br>703.9 OIII | |
| 708.3 | 709.2 AV | 707.3 OIII | |
| 716.0 | 715.6 AV<br>715.7 AV | | |
| 718.5 | 718.5 OII<br>718.6 OII | 718.1 AII | |
| 725.5 | 725.5 AII | | |
| 730.9 | 730.9 AII | | |
| 754.7 | 754.2 AIV<br>755.2 AIV | 754.8 AII | |
| 760.7 | 758.7 OV<br>759.4 OV<br>760.2 OV | 760.5 AIV<br>761.5 AIV | |

Table II (continued)

| Nominal λ(Å) | Tabulated spectral lines (Å) | |
|---|---|---|
| 760.7 | 760.5 OV | 762.2 AII |
| | 761.1 OV | |
| | 762.0 OV | |
| 764.3 | 763.3 NIII | 765.1 NIV |
| | 764.4 NIII | |
| 771.3 | 771.5 NIII | 769.2 AIII |
| | 771.9 NIII | |
| | 772.4 NIII | |
| 773.5 | 772.9 NIII | 774.5 OV |
| | 773.0 NIII | |
| 776.0 | 776.0 NII | |
| 780.0 | 779.8 OIV | |
| | 779.9 OIV | |
| 787.7 | 787.7 OIV | |
| 790.2 | 790.1 OIV | |
| | 790.2 OIV | |
| 796.7 | 796.7 OII | |
| 801.6 | 802.2 OIV | 800.6 AIV |
| | 802.3 OIV | 801.1 AIV |
| | | 801.4 AIV |
| | | 801.9 AIV |
| 807.9 | 806.9 AI | 807.7 AI |
| | 807.0 AI | 809.9 AI |
| 816.4 | 816.2 AI | |
| | 816.5 AI | |
| 823.8 | 822.2 AV | |
| | 825.4 AI | |
| 826.9 | 827.0 AV | 826.4 AI |
| | 827.4 | |

Table II (continued)

| Nominal λ(Å) | Tabulated spectral lines (Å) | | |
|---|---|---|---|
| 834.2 | 834.4 AI | 832.8 OII | 832.9 OIII |
| | 835.0 AI | 833.3 OII | 833.7 OIII |
| | | | 835.1 OIII |
| | 834.9 AV | 834.5 OII | 835.3 OIII |
| 840.0 | 840.0 AIV | | |
| 843.8 | 843.8 AIV | | |
| 850.6 | 850.6 AIV | | |
| 859.8 | 860.2 NI | 859.4 NI | |
| | 860.9 NI | 858.8 NI | |
| 864.5 | 866.8 AI | 862.2 NI | 863.2 NI |
| | | 862.9 NI | 864.9 NI |
| | | 865.6 NI | 865.9 NI |
| 871.1 | 871.1 AIII | 871.1 OIII | |
| 875.6 | 875.5 AIII | 875.5 OIII | |
| | 876.1 AI | 875.1 NI | |
| | | 875.3 NI | |
| 879.4 | 879.6 AIII | 880.0 AI | |
| | 878.7 OIII | | |
| 883.1 | 883.2 AIII | 882.9 OI | |
| 887.4 | 887.4 AIII | 887.4 OIII | |
| 892.2 | 894.3 AI | 890.0 OIII | |
| 901.1 | 900.4 AIV | 901.8 AIV | |
| | 901.2 AIV | | |
| 906.4 | 906.2 NI | 906.6 NI | |
| | 906.4 NI | | |
| 908.1 | 907.3 NI | 908.8 NI | |
| | 908.2 NI | | |
| 916.1 | 915.6 NII | 916.0 NII | |
| | 916.0 NII | 916.7 NII | |

Table II (continued)

| Nominal λ(Å) | Tabulated spectral lines (Å) | | | |
|---|---|---|---|---|
| 921.0 | 918.8 AII | 922.0 NIV | | |
| | 919.8 OII | 922.5 NIV | | |
| 923.5 | 923.1 NIV | 923.4 OIV | | |
| | 923.2 NIV | | | |
| | 923.7 NIV | | | |
| | 924.3 NIV | | | |
| 932.1 | 932.1 AII | | | |
| 937.2 | 936.6 OI | | | |
| | 937.8 OI | | | |
| 952.7 | 952.4 OI | 951.1 NI | 952.3 NI | 953.7 NI |
| | 952.9 OI | 951.4 NI | 952.5 NI | 954.0 NI |
| | | 952.8 NI | 953.4 NI | 953.4 NI |
| 956.8 | 958.3 AII | 955.3 NIV | | |
| 964.5 | 964.0 NI | 965.0 NI | | |
| | 964.6 NI | | | |
| 971.7 | 961.7 OI | | | |
| 973.4 | 973.2 OI | | | |
| | 973.9 OI | | | |
| 977.7 | 976.5 OI | 978.6 OI | | |
| | 978.0 OI | | | |
| 979.9 | 979.8 NIII | | | |
| | 979.9 NIII | | | |
| 989.0 | 988.6 OII | 988.8 OI | | |
| | 988.7 OII | 989.8 NIII | | |
| 990.8 | 990.1 OI | 991.5 NIII | | |
| | 990.0 OI | 991.6 NIII | | |
| | 990.8 OI | | | |
| 995.0 | | | | |
| 1004.0 | 1002.1 AIII | 1006.0 NIII | | |

Table II (continued)

| Nominal λ(Å) | Tabulated spectral lines (Å) | |
|---|---|---|
| 1008.9 | 1008.9 NI | |
| 1014.0 | | |
| 1018.0 | | |
| 1027.1 | 1025.8 OI<br>1027.4 OI | 1028.2 OI |
| 1040.6 | 1039.2 OI<br>1040.9 OI | 1041.7 OI |
| 1043.9 | 1043.1 NI<br>1043.6 NI | 1044.1 NI<br>1044.7 NI |
| 1048.2 | 1048.2 AI | 1048.2 OI |
| 1060.0 | | |
| 1067.2 | 1066.6 NI<br>1067.6 NI<br>1067.0 NI<br>1068.5 NI<br>1067.3 NI | 1066.7 AI<br>1066.7 OI |
| 1071.7 | 1071.7 NI | |
| 1078.0 | | |
| 1084.8 | 1085.7 NII<br>1084.6 NII | 1084.8 NII |

Table IV

| Type | Location | Symbol | Theoretical Energy | Exp. Energy |
|---|---|---|---|---|
| $M_o$ | (0, 0, 0) | $\Gamma_{25'} \rightarrow \Gamma_{2'}$ | 0.6 e.v. | 0.8 |
| $M_o$ | (0.5, 0.5, 0.5) | $L_{3'} \rightarrow L_1$ | 1.8 | 2.1 |
| $M_1$ | (0.17, 0.17, 0.17) | $\Lambda_3 \rightarrow \Lambda_1$ | 2.0 | 2.3 |
| $M_1$ | (1.0, 0, 0) | $X_4 \rightarrow X_1$ | 3.6 | 4.3 |
| $M_2$ | (0.61, 0.61, 0) | $\Sigma_4 \rightarrow \Sigma_1$ | 3.8 | 4.4 |
| $M_o$ | (0, 0, 0) | $\Gamma_{25'} \rightarrow \Gamma_{15}$ | 3.6 | 3.2 |
| $M_1$ | (0.56, 0.56, 0.39) | . . . | 5.3 | 5.6 |
| $M_2$ | (0.5, 0.5, 0.5) | $L_{3'} \rightarrow L_3$ | 5.4 | 5.7 |

IMPORTANT CRITICAL POINTS IN INTERBAND TRANSITIONS BELOW 6 e.v. FOR Ge

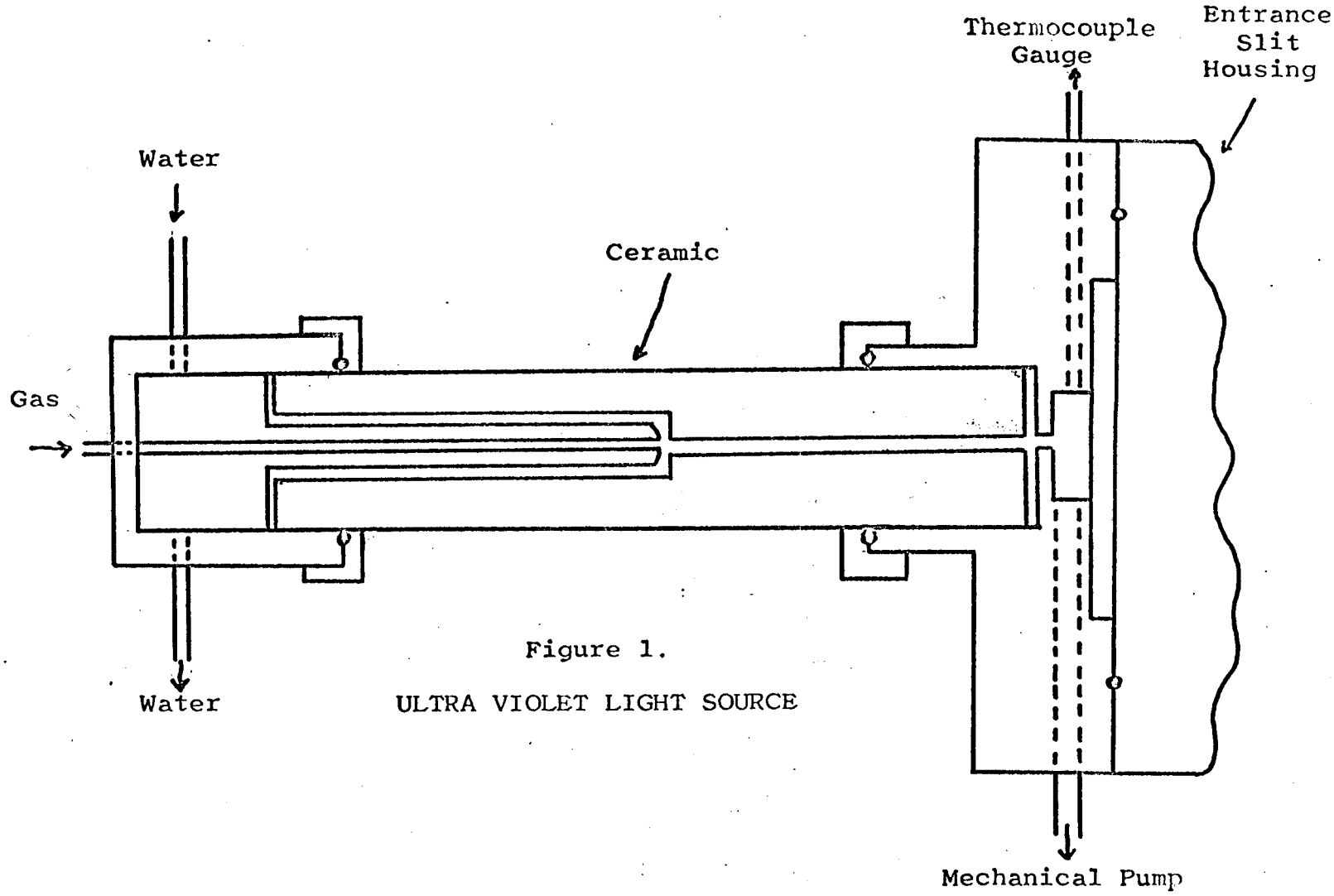


Figure 1.

ULTRA VIOLET LIGHT SOURCE

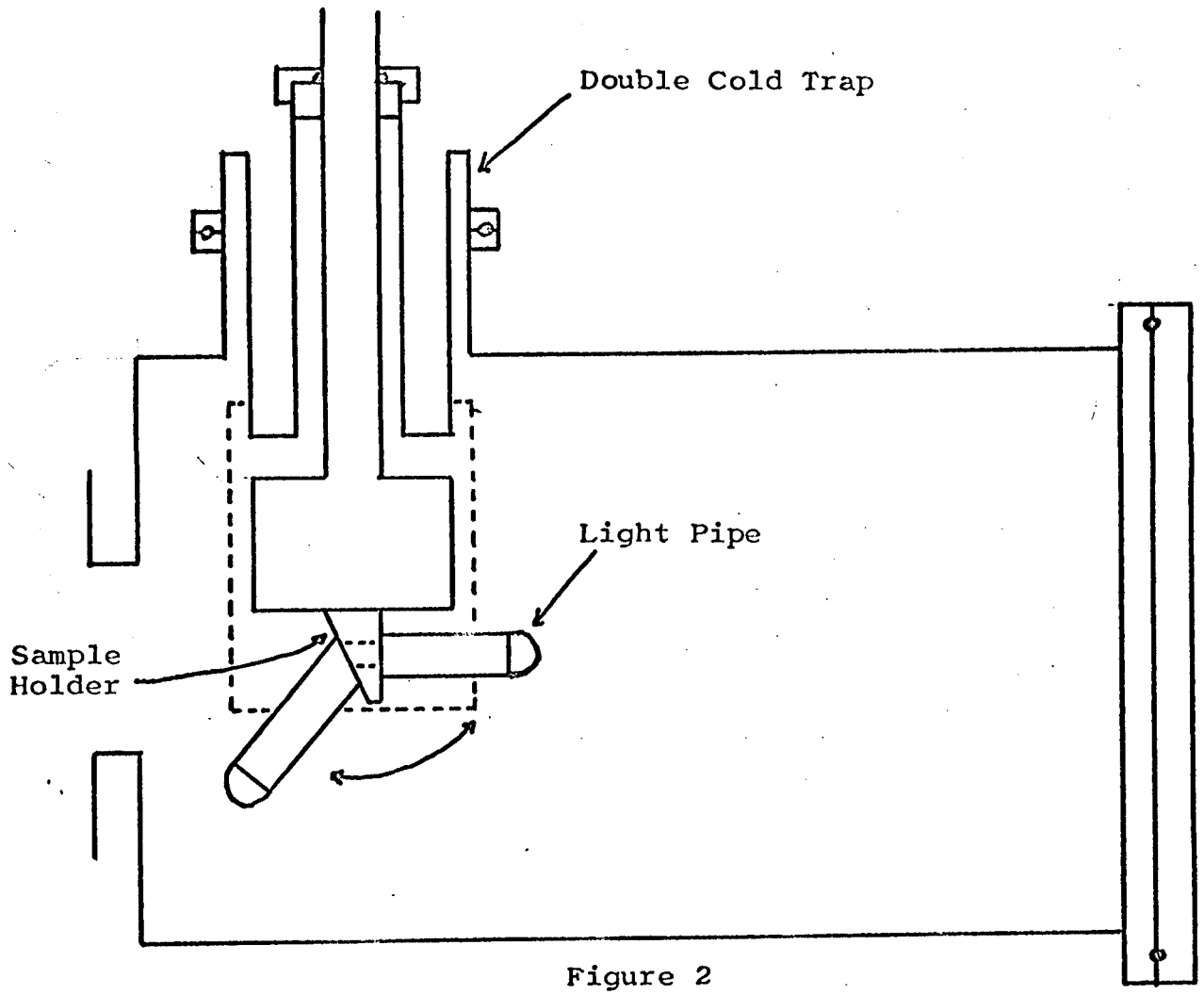


Figure 2

Side View Reflectometer

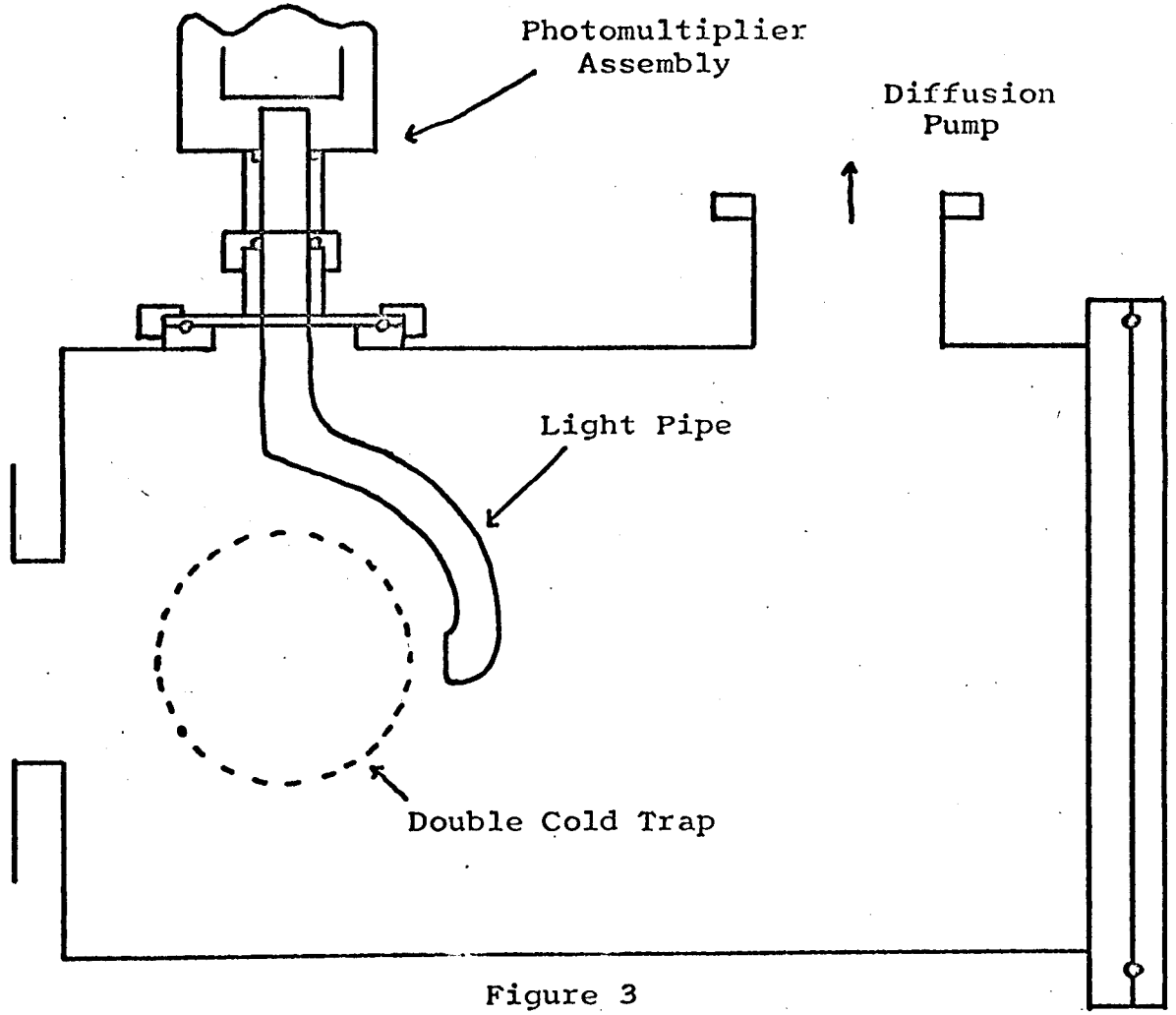


Figure 3

Top View Reflectometer

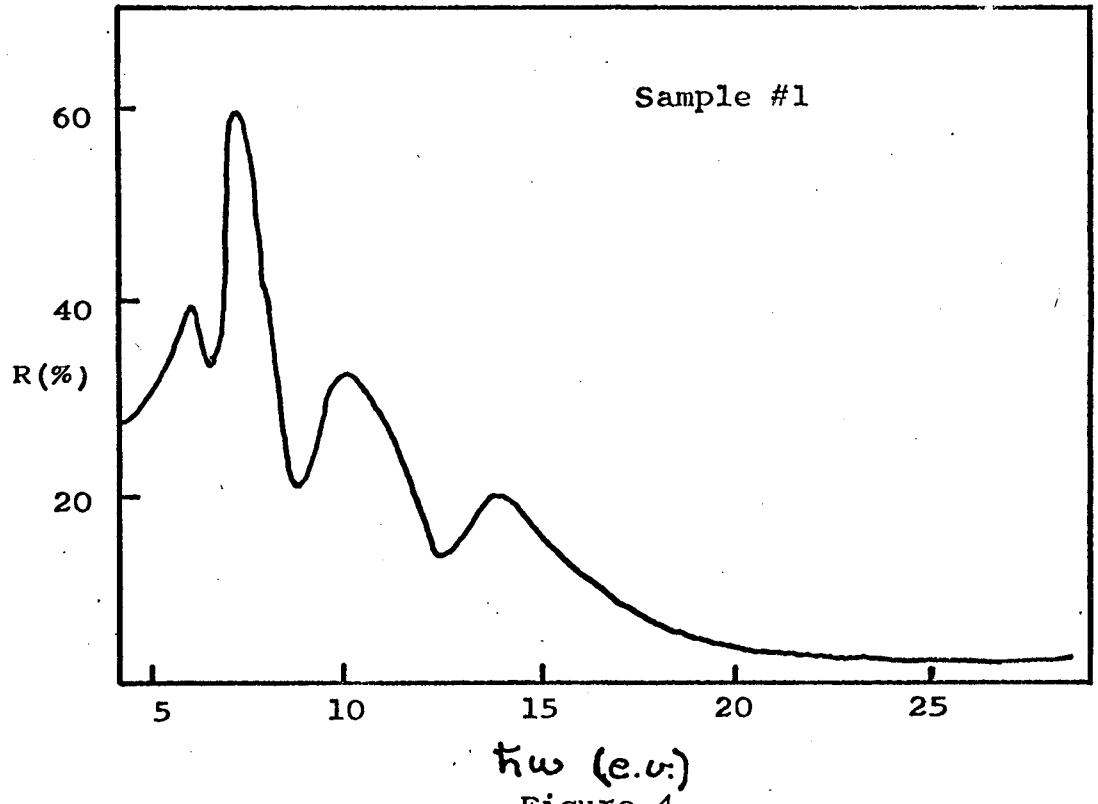


Figure 4

REFLECTION SPECTRUM OF CUBIC ZnS

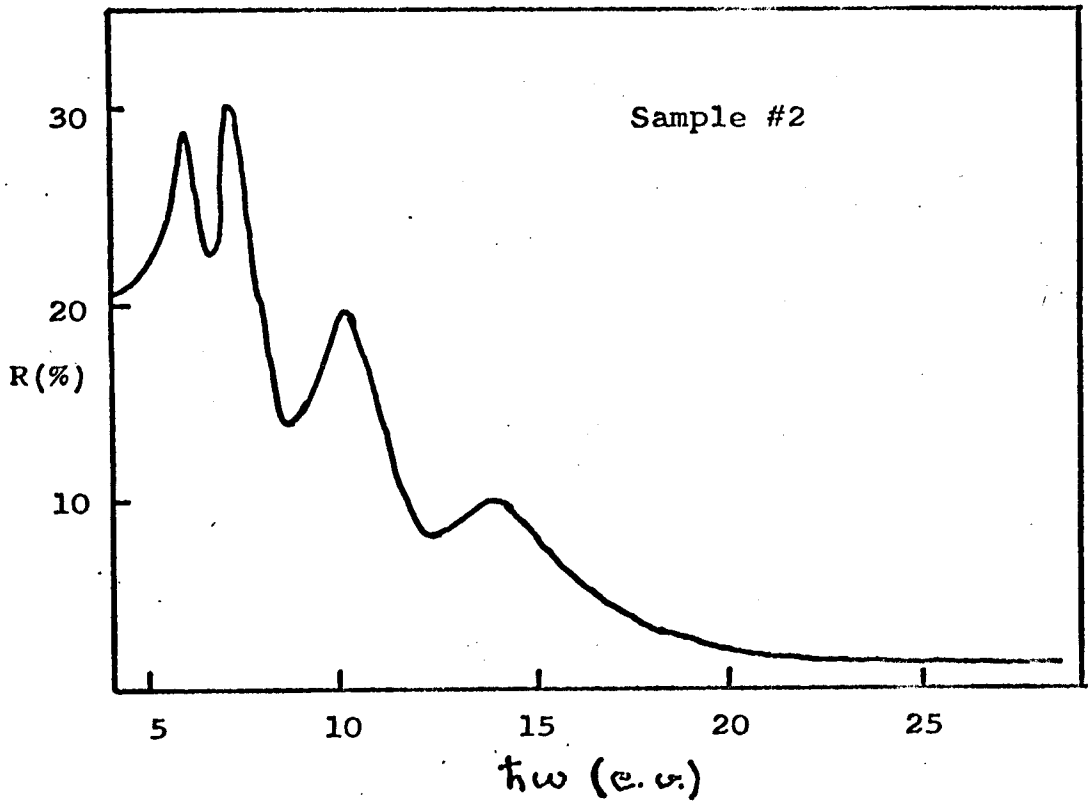


Figure 5

REFLECTION SPECTRUM OF CUBIC ZnS

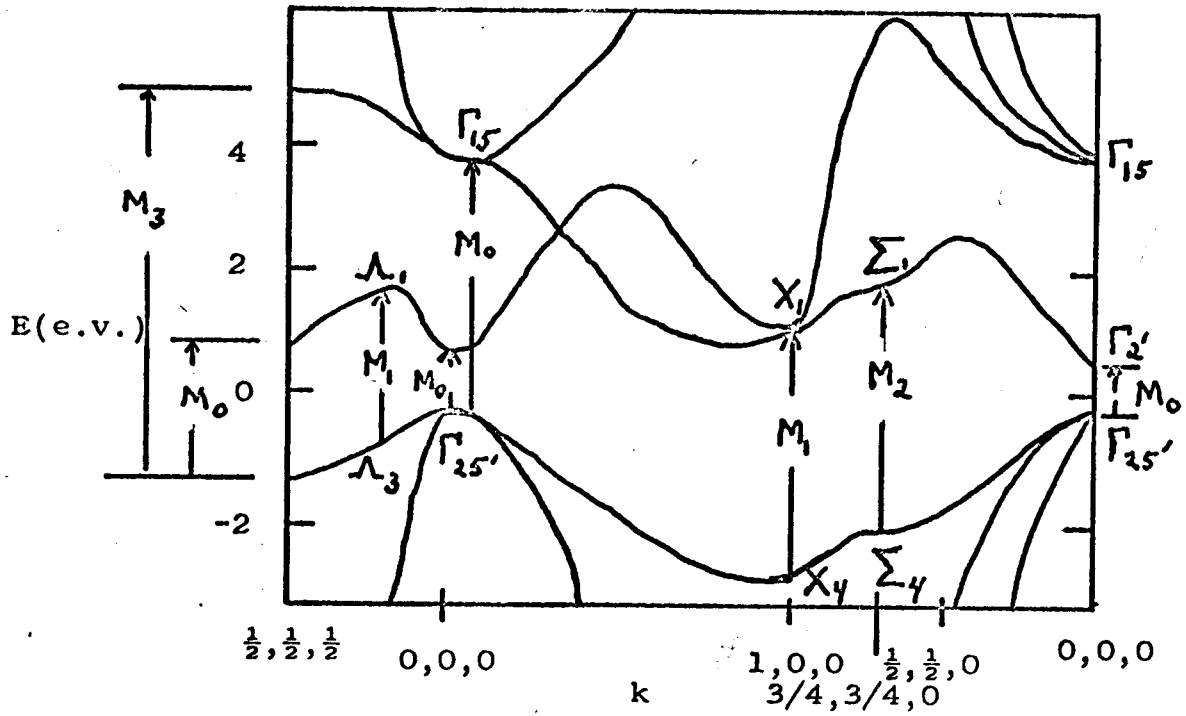


Figure 7

ENERGY BANDS FOR Ge.

IMPORTANT CRITICAL POINTS IN THE INTERBAND TRANSITIONS ARE INDICATED

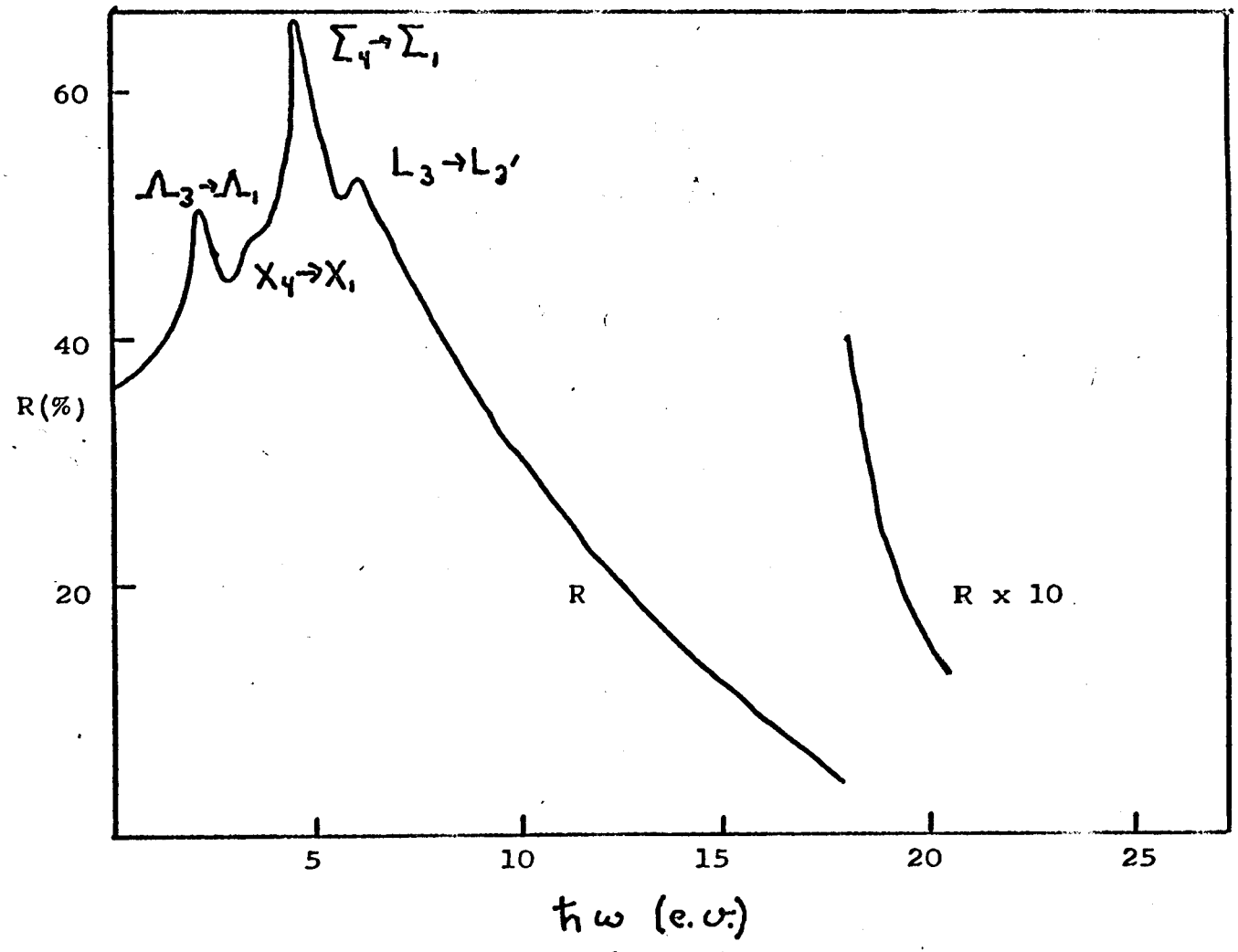


Figure 6

REFLECTION SPECTRUM OF SINGLE CRYSTAL Ge

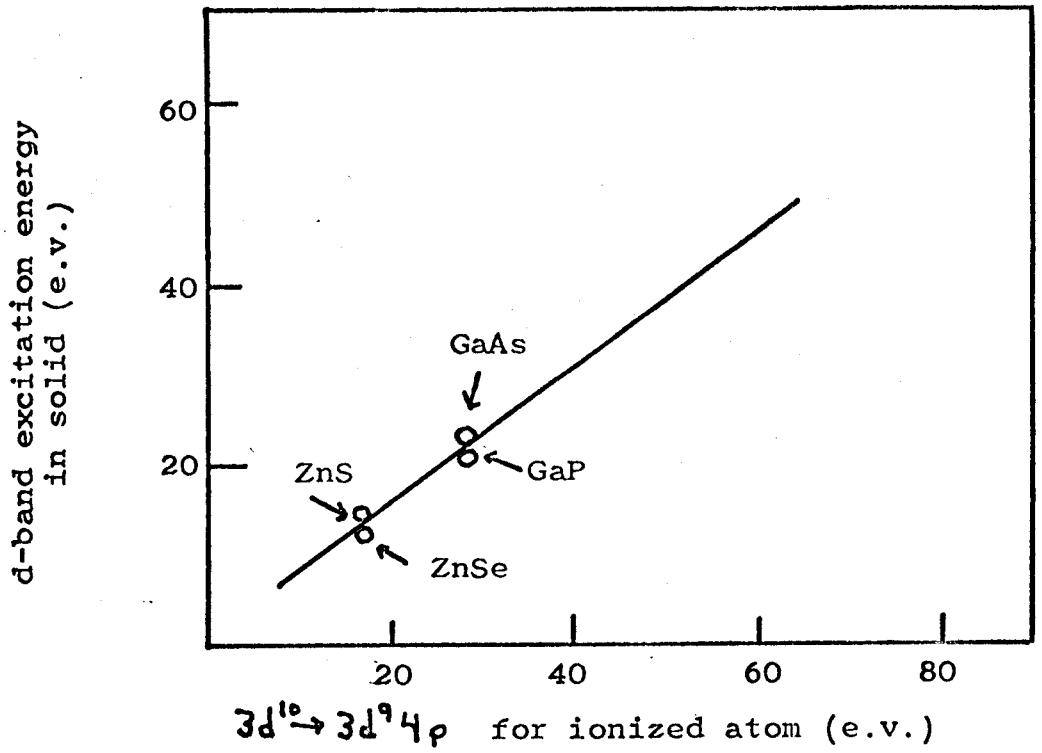


Figure 8

d-band ABSORPTION PEAKS VS. ATOMIC d-band TRANSITIONS

## REFERENCES


1. F. Herman and S. Skillman, Proceedings of the International Conference on Semiconductor Physics, Prague, 1960 (Czechoslovakian Academy of Sciences Publishing House, Prague, 1961), p. 20.

2. F. C. Jahoda, Reflectivity of Barium Oxide Single Crystals (Ph.D. Thesis), Cornell University, 1957.

3. H. Ehrenreich, H. R. Philipp, and J. C. Phillips, Phys. Rev. Letters, 8, 59 (1962).

4. H. R. Philipp, H. Ehrenreich, Phys. Rev., 129, 1550 (1963).

5. M. Cardona, Suppl. J. Appl. Phy., 32, 2151 (1961).

6. N. Wainfan, W. C. Walker, and G. L. Weissler, J. Appl. Phy., 24, 1318 (1953).

7. R. L. Kelly, Vacuum Ultraviolet Emission Lines. Livermore, California, University of California, Lawrence Radiation Laboratory, n.d.

8. Abbott Smith, Investigations of Photoconductivity and Photo-emission in Lead Sulphide (Ph.D. Thesis), University of Rochester, 1961.

9. W. C. Walker, Absolute Photoelectric Yield of Several Metals in the Vacuum Ultraviolet (Ph.D. Thesis), University of Southern California, 1955.

10. T. S. Moss, Optical Properties of Semi-Conductors. Butterworths Scientific Publications, London, 1959.

11. F. Seitz, Modern Theory of Solids, (New York, McGraw-Hill, 1940), Chapter 17.

12. R. A. Smith, Wave Mechanics of Crystalline Solids, (New York, Wiley, 1961), p. 403ff.

13. D. Brust, J. C. Phillips, and F. Bassani, Phys. Rev. Letters, 9, 94 (1962).

14. W. C. Walker, J. Osantowski, J. Opt. Soc. Am., 53, 399 (1963).

15. H. R. Philipp and H. Ehrenreich, Phys. Rev. Letters, 8, 92 (1962).